Biochemistry and Biophysics Reports 38 (2024) 101733

Contents lists available at ScienceDirect

Biochemistry and Biophysics Reports

journal homepage: www.elsevier.com/locate/bbrep

Epigenome editing revealed the role of DNA methylation of T-DMR/CpG island shore on Runx2 transcription

Yutaro Kawa [a], Miyuki Shindo [b], Jun Ohgane [c], Masafumi Inui [a,*]

[a] Laboratory of Animal Regeneration Systemology, Department of Life Sciences, School of Agriculture, Meiji University, Kanagawa, 214-8571, Japan
[b] Division of Laboratory Animal Resources, National Research Institute for Child Health and Development, 2-10-1 Okura, Setagaya, Tokyo, 157-8535, Japan
[c] Laboratory of Genomic Function Engineering, Department of Life Sciences, School of Agriculture, Meiji University, Kanagawa, 214-8571, Japan

ARTICLE INFO

Keywords:
Epigenome editing
Runx2
Differentially methylated region
Osteoblast
CpG island shore

ABSTRACT

RUNX2 is a transcription factor crucial for bone formation. Mutant mice with varying levels of *Runx2* expression display dosage-dependent skeletal abnormalities, underscoring the importance of *Runx2* dosage control in skeletal formation. RUNX2 activity is regulated by several molecular mechanisms, including epigenetic modification such as DNA methylation. In this study, we investigated whether targeted repressive epigenome editing including hypermethylation to the Runx2-DMR/CpG island shore could influence *Runx2* expression using Cas9-based epigenome-editing tools. Through the transient introduction of CRISPRoff-v2.1 and gRNAs targeting Runx2-DMR into MC3T3-E1 cells, we successfully induced hypermethylation of the region and concurrently reduced *Runx2* expression during osteoblast differentiation. Although the epigenome editing of Runx2-DMR did not impact the expression of RUNX2 downstream target genes, these results indicate a causal relationship between the epigenetic status of the Runx2-DMR and *Runx2* transcription. Additionally, we observed that hypermethylation of the Runx2-DMR persisted for at least 24 days under growth conditions but decreased during osteogenic differentiation, highlighting an endogenous DNA demethylation activity targeting the Runx2-DMR during the differentiation process. In summary, our study underscore the usefulness of the epigenome editing technology to evaluate the function of endogenous genetic elements and revealed that the Runx2-DMR methylation is actively regulated during osteoblast differentiation, subsequently could influence *Runx2* expression.

1. Introduction

Runt-related transcription factor 2 (RUNX2) is a transcription factor essential for osteogenesis that regulates the expression of osteogenic genes such as Osterix, Osteocalcin, and Bone sialoprotein [1]. *Runx2* homozygous knockout (KO) mice lack most of the mineralized bone, and its heterozygous KO mice display skeletal abnormalities, including delayed closure of cranial suture and hypoplasia of clavicles [2,3]. Mutation in the human *RUNX2* gene causes cleidocranial dysplasia (CCD), an autosomal dominant disorder in which skeletal abnormalities similar to those of *Runx2* heterozygous KO mice are observed [4]. The haploinsufficiency nature of *Runx2* indicates that this gene is not only essential for bone formation, but also that its dosage is closely associated with bone morphology. In line with this idea, transgenic mice overexpressing *Runx2* also showed abnormal bone morphology, and the mutant mice with the *Runx2* expression level at 70 % of that of wild type showed abnormal skeletal development [5,6]. As a quantitatively precise *Runx2* expression level is essential for normal bone formation, various mechanisms have been reported to regulate RUNX2 expression and activity [7].

DNA methylation around the *Runx2* locus has been associated with *Runx2* expression levels or osteoarthritis, in which *Runx2* plays roles in pathology, implying that this epigenetic regulation could be involved in *Runx2* expression as well as skeletal development [8,9]. Previously, a tissue-specific differentially DNA-methylated region (T-DMR) was identified in the Runx2 locus. This DMR is located between the transcription start sites of the two transcript variants, *Runx2-I* and *Runx2-II*, and the methylation rate inversely correlates with the *Runx2* expression during osteoblast differentiation (Fig. 1A and B) [10]. This region caught our interest because it is at the boundary between the highly methylated intergenic region and the CpG island with low methylation rate proximal to the *Runx2-I* TSS, i.e., the CpG island shore of the

* Corresponding author.
E-mail address: inui_m@meiji.ac.jp (M. Inui).

https://doi.org/10.1016/j.bbrep.2024.101733
Received 29 March 2024; Received in revised form 6 May 2024; Accepted 13 May 2024

Runx2-I gene. Because CpG island shores have often been subject to differential DNA methylation in tissue/cell-type-dependent and/or stochastic manners [11,12] in association with the transcriptional activity of the gene in the vicinity (Fig. 1A) [13,14], DNA methylation in the T-DMR/CpG island shore of *Runx2-I* may have a functional role in the quantitative regulation of *Runx2* expression. However, the causal relationship between DNA methylation of specific loci and the expression of specific adjacent genes has been elusive due to the lack of methodology for the direct intervention in DNA methylation at targeted regions. Recently, epigenome editing based on CRISPR/Cas9 technology has emerged. By directly fusing or indirectly assembling epigenetic effectors, such as DNA methyltransferase or transcriptional repressor, to nuclease-inactive Cas9 (dCas9), the epigenetic mark in the vicinity of the target site of gRNA can be artificially altered [15,16]. Recent studies indicated that the simultaneous recruitment of de novo DNA methyltransferase, such as DNMT3A/3L, and Krüppel-associated box (KRAB) domain induces heritable repressive epigenome editing at the target loci [17–19]. In this study, we aimed to elucidate whether targeted induction of a repressive epigenome editing to Runx2-DMR could affect the *Runx2* expression as well as the osteoblast differentiation, using the Cas9-based epigenome-editing technology CRISPRoff, a fusion protein of dCas9, DNMT3A/3L, and KRAB domain.

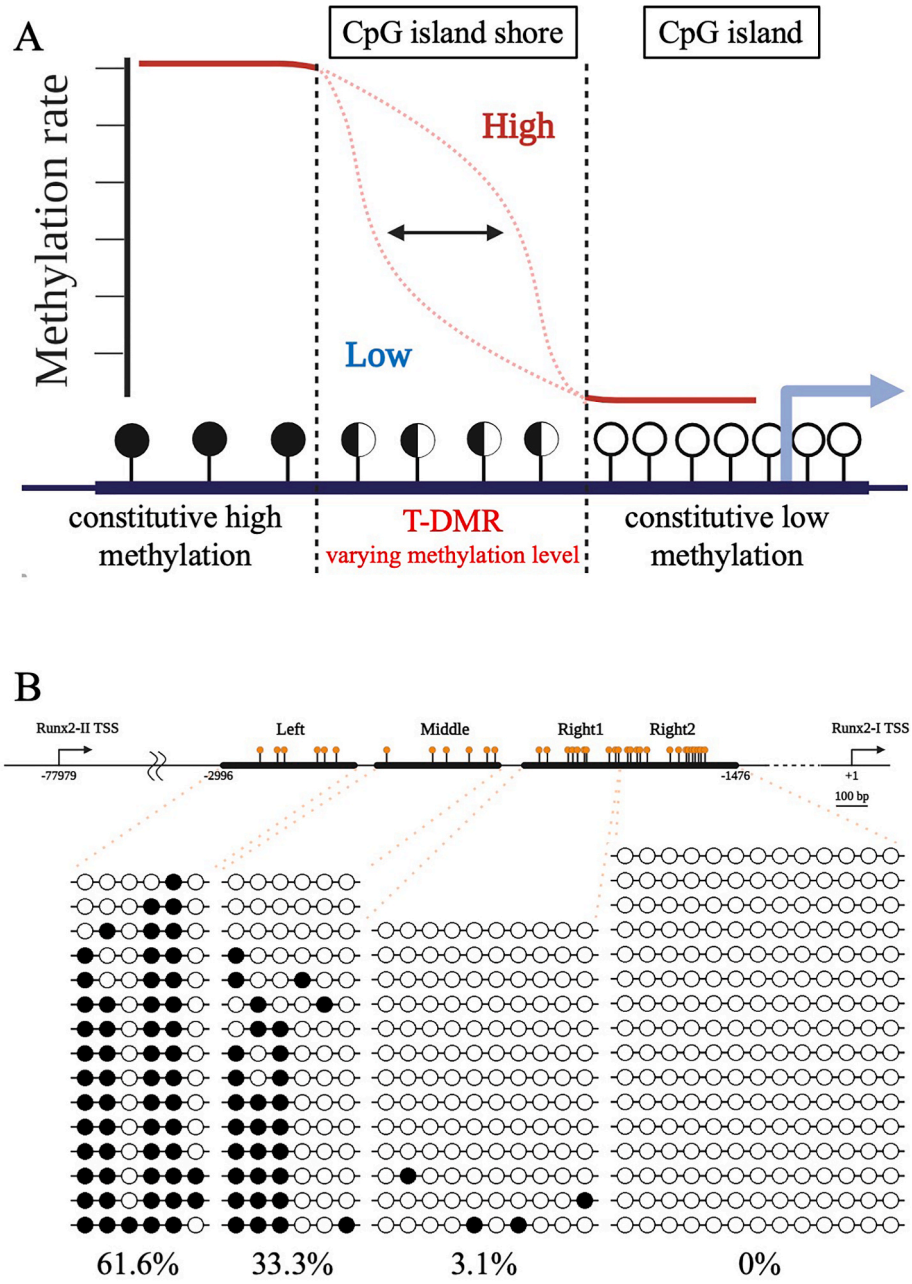

Fig. 1. DNA methylation status of Runx2-DMR in MC3T3-E1 cell (A) Conceptual diagram representing the DNA methylation variations of T-DMRs in CpG island shores. The upper red line illustrates the DNA methylation levels of each region. Circles in the lower part represent CpG sites, with black and white indicating methylated and unmethylated CpG, respectively. (B) Methylation analysis of Runx2-DMR in untreated MC3T3-E1 cells. The upper panel schematically illustrates Runx2-DMR where Left/Middle/Right1/Right2 regions were depicted by black bars and CpG sites were indicated by orange circles. Numbers at the bottom of the line indicate the distance from the Runx2-I TSS. The lower panel presents the result of the bisulfite sequence. Numbers at the bottom indicate the ratio of methylated CpG in each region in a single experiment shown in this Figure. Similar result was reproduced in one more independent experiment of which the result is shown in Fig. S1 (n = 2). (For interpretation of the references to colour in this figure legend, the reader is referred to the Web version of this article.)

2. Materials and methods

2.1. MC3T3-E1 cell cultures

MC3T3-E1 cells (RIKEN Cell Bank, RCB1126) were cultured in α-MEM (Nacalai Tesque, Kyoto, Japan) supplemented with 10 % fetal bovine serum (FBS; CELLECT, MP Biomedicals inc., CA, USA) and Penicillin-Streptomycin-Glutamine mixed solution (PSG, Nacalai Tesque), and incubated at 37 °C under 5 % CO_2. For differentiation induction, MC3T3-E1 cells were seeded in multi-well culture plates and the medium was changed to differentiation medium (α-MEM, 10 % FBS, 1 % PSG, and 10 mM β-glycerophosphate (FUJIFILM Wako, Osaka, Japan), 50 μg/ml ascorbic acid (FUJIFILM Wako), 50 ng/ml BMP-2 (PEPROTECH, NJ, USA)) at confluence. Then, the medium was changed to a differentiation medium without BMP-2 after 3 days. 200 μg/mL G418 bisulfate (Nacalai Tesque) was used for the selection.

2.2. Alizarin red staining

The cells were fixed with 500 μL of 10 % formalin solution for 15 min and stained with 500 μL of alizarin red S solution (0.04 M alizarin red S (SIGMA-ALDRICH, MO, USA), 0.001 % ammonium hydroxide (SIGMA-ALDRICH)) for 20 min. Stained alizarin red S was extracted by 10 % acetic acid solution and the absorbance at 405 nm was measured with Spectra max iD5, MOLECULAR DEVICES. The average of 3 wells (biological replica) were shown.

2.3. Fluorescence-Activated Cell Sorting (FACS)

Cells were detached by Trypsin EDTA treatment, centrifuged, and suspended in PBS. The suspension was aliquoted into a 5 mL test tube with a cell strainer cap (Corning, NY, USA) and sorted using Cell Sorter SH800S (SONY, Tokyo, Japan).

2.4. Reverse transcription-quantitative polymerase chain reaction (RT-qPCR)

RT-qPCR was performed as previously described [20]. Briefly, total RNA was isolated using ISOGEN-LS (NIPONGENE, Tokyo, Japan), according to the manufacturer's protocol. Total RNA was reverse-transcribed with oligo-d(T) primers and SuperScript II Reverse Transcriptase (Thermo Fisher Scientific, MA, USA). qPCR was performed using Power SYBR® Green Master Mix (Thermo Fisher Scientific). Primer sequences are shown in Table S1.

2.5. Primer design for bisulfite PCR

The genomic DNA sequence of interest was obtained from the UCSC Genome Browser and bisulfite PCR primer sets for amplifying regions below were designed using MethPrimer [21]. Target regions were set as, Left region: chr17:44,739,211–44,739,644, Middle region: chr17:44,738,770–44,739,169, Right1 region: chr17:44,738,375–44,738,695, Right2 region: chr17:44,738,124–44,738,397). Primer sequences are shown in Table S1.

2.6. DNA methylation analysis

Cells were detached by Trypsin EDTA treatment, centrifuged, and genomic DNA was extracted from the cell pellet using NucleoSpin® Tissue (Takara, Shiga, Japan) according to the manufacturer's protocol. Bisulfite conversion and subsequent DNA methylation analysis were performed as previously described [12]. Briefly, genomic DNA (500 ng–1000 ng) was subjected to bisulfite reactions using Epitect Bisulfite Kits (QIAGEN, Venlo, Netherland) according to the manufacturer's protocol. Following bisulfite conversion, genomic DNA was amplified by PCR using GoTaq® Master Mixes (Promega, WI, USA). PCR products were cloned into the pGEM-T Easy vector (Promega). PCR products of colony PCR were sequenced. DNA sequencing and methylation data were visualized using QUMA software [22].

2.7. Plasmid construction and gRNA design

EGFP and dsRED expression cassettes were inserted into the NotI site of CRISPRoff-v2.1 [18] (Addgene ID: #167981). EGFP expression cassette was inserted into the SnaBI site of the gRNA cloning vector + adaptor [23,24]. gRNAs were designed using CRISPRdirect [25] and cloned as described [23]. gRNA positions along with Runx2-DMR are shown in Fig. S1 and gRNA sequences are shown in Table S1. All the plasmids constructed were sequenced.

3. Results

3.1. Methylation analysis of the Runx2-DMR in MC3T3-E1 cells

To explore the effect of epigenome editing on the mouse Runx2-DMR (referred to in this manuscript as GRCm39/mm39 chr17:45046900–45048900), we first established the conditions for methylation analysis of this region in MC3T3-E1 cells. Wakitani et al. focused on CpGs ranging from −3371 to −2039 bp relative to the TSS of *Runx2-I* and divided it into three regions: Left, Middle, and Right, which we further subdivided into Right1 and Right2 (Fig. 1B). The bisulfite sequencing analysis revealed that the methylation rates of the Left, Middle, Right1, and Right2 regions were 65.2 ± 3.6 %, 30.2 ± 3.1 %, 3.1 ± 0 %, and 1.5 ± 1.5 % during the exponential growth phase of MC3T3-E1 cells (Fig. 1B, Fig. S1). A high DNA methylation rate in the upstream regions and a low methylation rate in downstream regions confirm the "CpG island shore" characteristics of this region. Moreover, the DNA methylation rate of this region in MC3T3-E1 cells was similar to that of previously reported in mouse bone tissues [10], supporting our aim to use this cell line to gain insight into the in vivo osteogenic process.

3.2. Design of gRNAs for Runx2-DMR and epigenome editing using G418 selection

Next, we investigated whether the transient introduction of an epigenome editing construct could modulate the methylation pattern of Runx2-DMR in MC3T3-E1 cells. We designed three gRNAs (gRNA-1, 2, and 3) targeting this region (Fig. 2A, Fig. S2 and see methods for design criteria) and introduced them to MC3T3-E1 cells either singly or in a pool, along with the CRISPRoff vector. A gRNA vector lacking the target recognition sequence (hereafter "empty") served as the control. After the plasmid transfection and a 4-day G418 selection, the cells were allowed to grow until day 11 post-transfection, at which point methylation analysis was performed (Fig. 2B). The methylation rates in the "empty" control sample, were similar to those in non-transfected MC3T3-E1 cells (Fig. 2C, Fig. S3: Left region, 61.45 % ± 1.05 %; Middle region, 43.4 % ± 4.5 %; Right1 region, 2.65 % ± 0.45 %; Right2 region, 4.65 % ± 0.35 %). Conversely, the methylation rates in samples transfected with gRNA1, 2, and 3 showed substantial changes in the target regions (Fig. 2C, Fig. S3). The methylation rates of the R1 region in CRISPRoff/gRNA1-expressed cells increased to 18.65 % ± 6.85 %, while those of the Left, Middle, and R2 regions remained at similar to or lower than the control sample (Fig. 2C, Fig. S3). Similarly, the DNA methylation rates of the R1 and R2 regions in CRISPRoff/gRNA2-expressed cells (12.8 % ± 3.3 % and 25.7 % ± 8.3 %, respectively) and CRISPRoff/gRNA3-expressed cells (15.8 % ± 8.3 % and 14.9 % ± 1.3 %, respectively) were higher compared to the "empty" control sample. In cells where gRNA1, gRNA2, and gRNA3 were co-transfected (hereafter "pooled" sample), the R1 and R2 regions exhibited higher methylation rates compared to the "empty" control, with rates of 12.55 % ± 3.95 % and 33.7 % ± 9.7 %, respectively (Fig. 2C, Fig. S3). These results

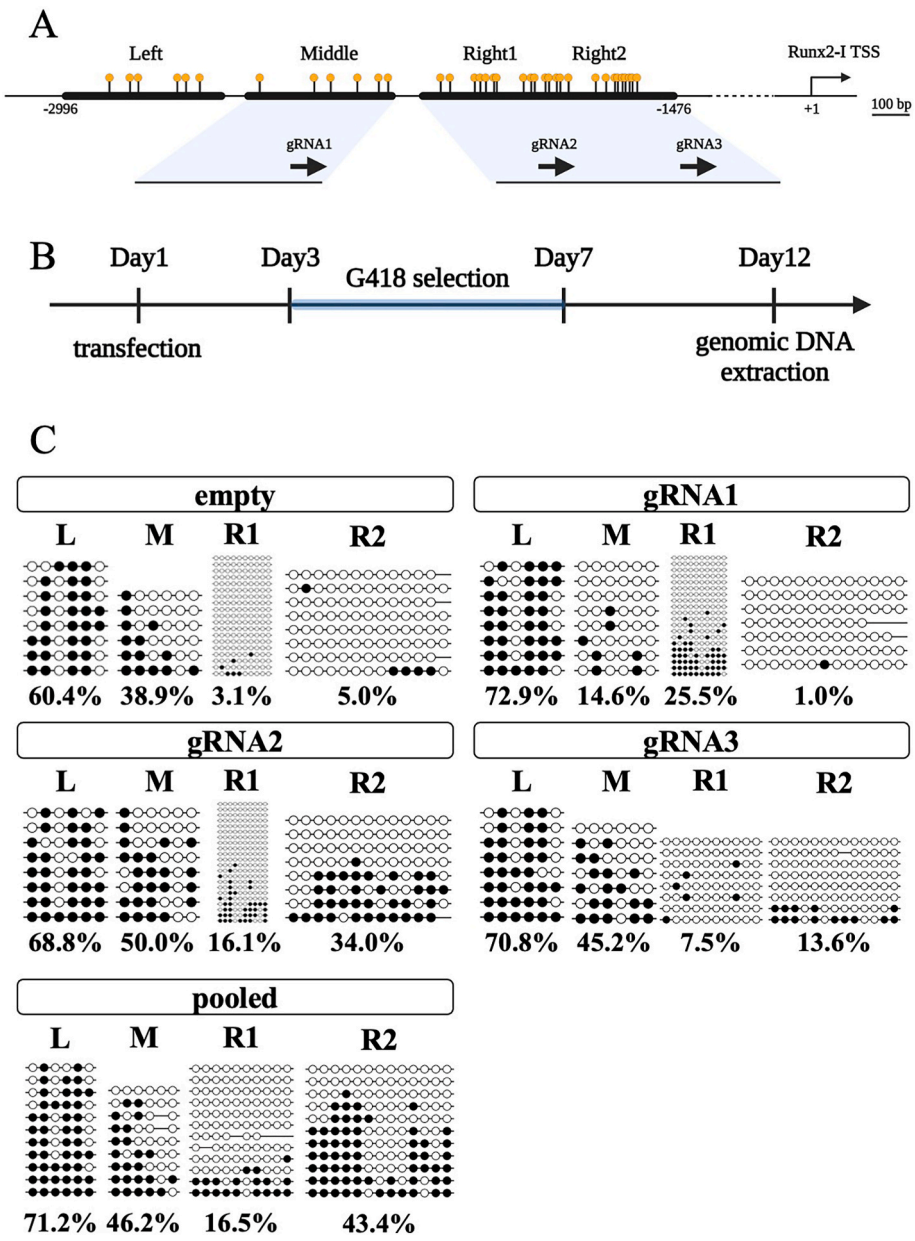

Fig. 2. Epigenome editing of Runx2-DMR using G418 selection (A) A schematic drawing illustrating the positions of gRNAs targeting Runx2-DMR, which are shown in black arrows at the bottom. The PAM sequences are on the arrowhead sides. (B) The time course of the DNA methylation analysis of the Runx2-DMR using G418 selection. (C) The result of DNA methylation analysis. gRNAs introduced in each sample are shown on the top. The analyzed regions are denoted as L: Left, M: Middle, R1: Right1, R2: Right2. Numbers at the bottom indicate the ratio of methylated CpG in each region in a single experiment shown in this Figure. Similar result was reproduced in one more independent experiment of which the result is shown in Fig. S3 (n = 2).

demonstrated that the introduction of CRISPRoff and gRNAs into MC3T3-E1 cells could increase DNA methylation rates in the vicinity of the gRNA target sites within the Runx2-DMR. We observed that the CRISPRoff-induced DNA hypermethylation peaked approximately 100–200 bp away from each of the gRNA target site and was limited to a region of 200–300 bp in length (Fig. S2). However, DNA hypermethylation covered the entire R1/R2 regions in the "pooled" sample while retaining a methylation level similar to that in single gRNA-induced samples (Fig. 2C). Based on these findings, we opted to use the gRNA1/2/3 "pooled" setup for further experiments and focus primarily on the R1 and R2 regions to evaluate of methylation status of Runx2-DMR.

3.3. Optimizing selection conditions

While the results so far indicated that our epigenome editing setup was qualitatively effective, the extent of DNA methylation change was around 20 %–30 %, which might be insufficient to significantly alter the transcriptional level of *Runx2*. We observed that the increased methylation level in CRISPRoff/gRNA-transfected cells reflected a few highly methylated alleles, yet a substantial number of alleles remained at the same methylation level as that of control cells (e.g. the 25.5 % methylation rate in the R1 region of CRISPRoff/gRNA1-transfected cells depended on 5 highly methylated alleles out of 20, Fig. 2C). Our previous data has indicated that each cloned and sequenced fragment from bisulfite sequencing could be considered as representing one of the two alleles in a cell [12,26], leading us to consider that the unaffected alleles might result from non-transfected or editing-insufficient

low-copy-number-transfected cells that remained after the G418 selection. To overcome this limitation, we employed Fluorescence-Activated Cell Sorting (FACS) to achieve more efficient epigenome editing. Because the fluorescence signal of TagBFP in the CRISPRoff vector was insufficient for sorting MC3T3-E1 cells, we co-transfected an EGFP expression vector, inserted an EGFP expression cassette into the CRISPRoff vector, or into the gRNA vectors and sorted GFP-positive cells by FACS (Fig. 3A). However, the methylation rates of R1 and R2 regions remained lower than 30 % in cells selected under these conditions (Fig. 3B, C, Fig. S4). Given these results, we introduced expression cassettes of EGFP and dsRED into the CRISPRoff vector and the gRNA cloning vector, respectively, and sorted for EGFP/dsRED double-positive cells. As a result, the DNA methylation rates in the Middle, Right1, and Rignt2 regions were 47.9 %, 58.2 %, and 66.3 %, respectively (Fig. 3B–D). Based on these results, we determined this double-positive sorting as the preferred selection method for further analyses.

3.4. Effects of Runx2-DMR epigenome editing on gene expression and osteoblast differentiation

Subsequently, we examined the impact of epigenome editing of the Runx2-DMR on *Runx2* expression and its role in osteoblast differentiation. CRISPRoff and gRNA vectors were transfected into MC3T3-E1 cells on Day 1, FACS sorted on Day 3, and differentiation induction was initiated on Day 10. The DNA methylation rates of Runx2-DMR, as well as gene expression were evaluated before and after the 14 days of differentiation period (Fig. 4A). At differentiation Day 0 (= Day 10 after the transfection), the DNA methylation rates in the Right1 and Right2 regions significantly increased in the "pooled" sample (56.5 % ± 0.4 % and 38.75 % ± 2.35 %) compared to the control "empty" sample (5.15 % ± 2.45 % and 9.45 % ± 0.25 %) as the previous experiments. However, at differentiation Day 14, the DNA methylation rates of the "pooled" sample were decreased to 24.25 % ± 2.65 % in R1 and 20.6 % ± 4.9 % in R2 region while those of the control "empty" sample remained at similar level to differentiation Day 0 (Fig. 4, Fig. S5A). To examine

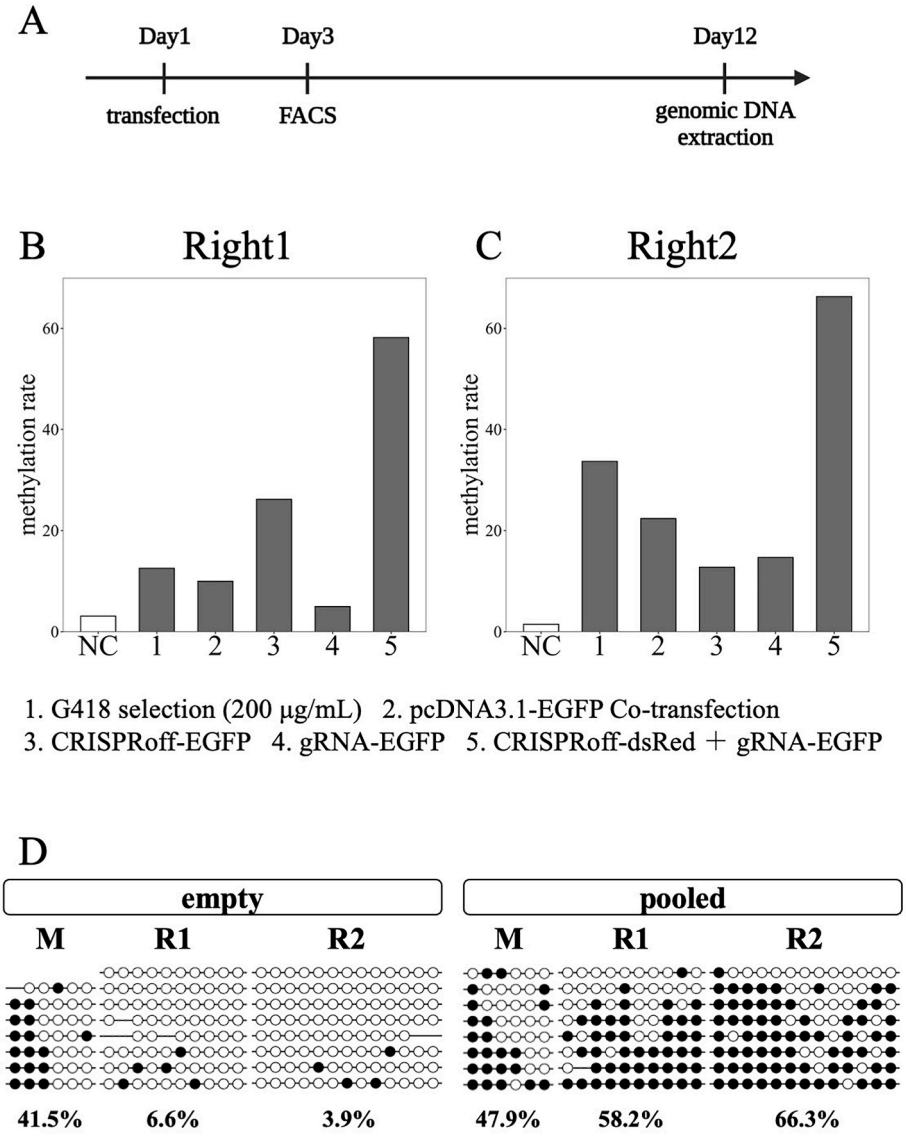

Fig. 3. Optimization of Runx2-DMR epigenome editing using FACS (A) The time course of the DNA methylation analysis of the Runx2-DMR using FACS sorting. (B, C) DNA methylation rates of the Right1 and Right2 regions of the cells selected through various conditions. Five conditions for selection are shown at the bottom. NC: no treatment. (D) The bisulfite sequence results of selection condition 5. M: Middle, R1: Right1, and R2: Right2 regions. The DNA methylation analyses were performed once for condition 1–4 (n = 1) for screening, and twice for condition 5 (n = 2) to confirm relatively high methylation state by this method. Essentially the same results were obtained in a reproductive experiment and the result is shown in Fig. S4.

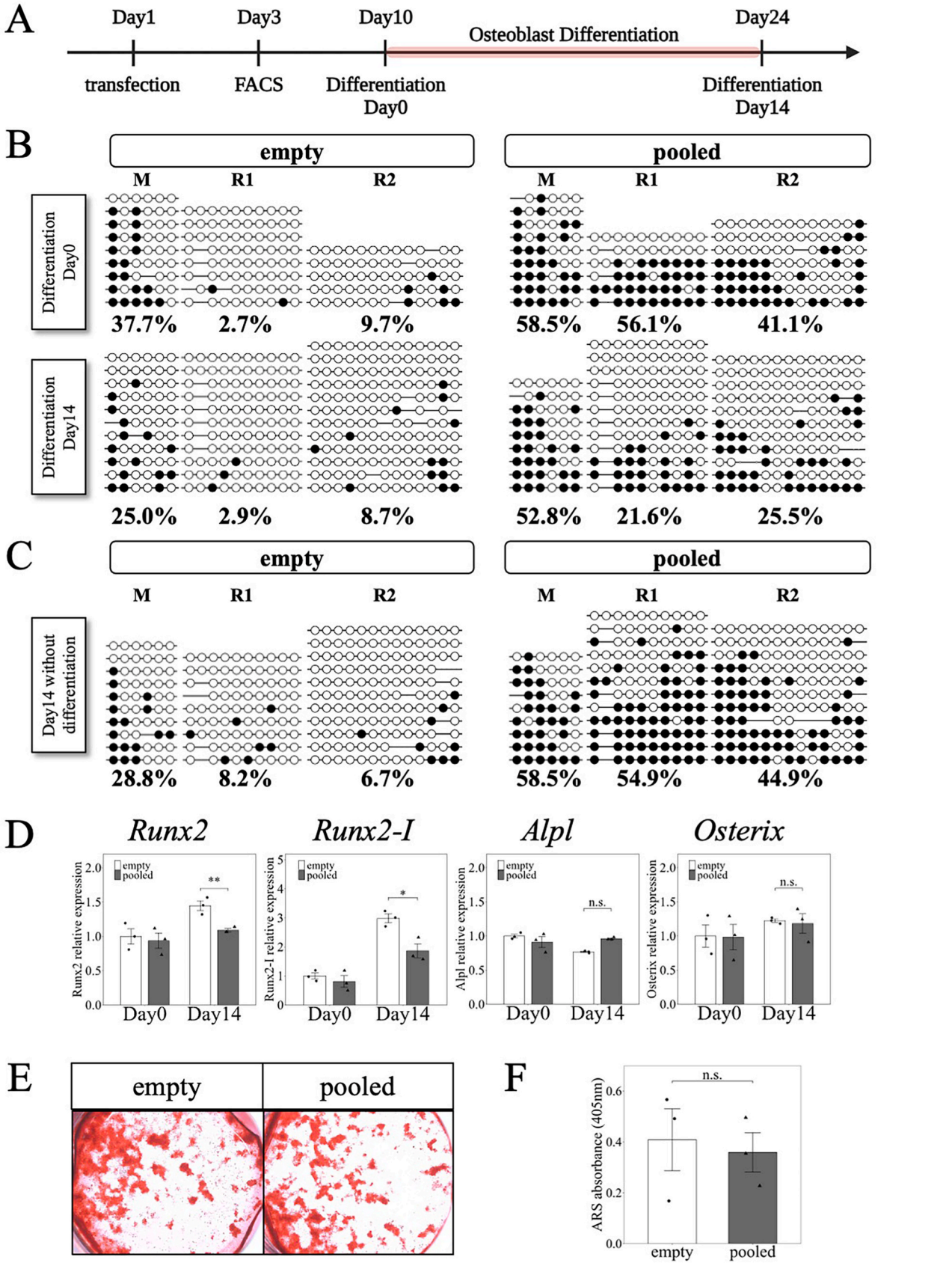

(caption on next page)

Fig. 4. Effects of Runx2-DMR epigenome editing on gene expression and osteoblast differentiation (A) The time course of the epigenome editing and differentiation analysis. (B, C) The DNA methylation analysis for the control ("empty") and gRNA1,2,3-transfected cells ("pooled") at Differentiation Day 0, Differentiation Day 14, and Day 24 without differentiation. The analyzed regions are denoted as M: Middle, R1: Right1, R2: Right2. Numbers at the bottom indicate the ratio of methylated CpG in each region in a single experiment shown in this Figure. Similar result was reproduced in one more independent experiment of which the result is shown in Fig. S5 (n = 2). (D) The gene expression analysis for control ("empty") and gRNA1,2,3-transfected cells ("pooled") at Differentiation Day 0 and Differentiation Day 14. The expression levels of each mRNA were normalized by that of GAPDH. The data were shown as mean ± SE and analyzed by Student's t-test. *$p < 0.05$, **$p < 0.01$. (E, F) The alizarin red S staining and its quantification for the control ("empty") and gRNA1,2,3-transfected cells ("pooled") at Differentiation Day 14. Triplicated wells for each condition showed similar staining levels and the representative images are shown. The quantification data were statistically analyzed using Student's t-test. Mean ± SE. *$p < 0.05$, **$p < 0.01$. experiments were performed twice and essentially the same results were obtained. The figure shows representative results. (For interpretation of the references to colour in this figure legend, the reader is referred to the Web version of this article.)

whether these reductions in DNA methylation rates are due to a passive DNA demethylation over time, or an active DNA demethylation process associated with osteoblast differentiation, we analyzed the DNA methylation status of "empty" and "pooled" samples after the same period of cultivation without differentiation induction. As a result, the DNA methylation rates in "pooled" samples remained high even after the 14 days of culture (52.4 % ± 6.1 % in the Middle region, 60.6 % ± 5.7 % in the Right1 region, and 43.05 % ± 1.85 % in the Right2 region, respectively) (Fig. 4C, Fig. S5B). These results clearly show that the DNA hypermethylation introduced by epigenome editing is stable, at least until 24 days post-transfection, and an endogenous DNA demethylation activity was imposed on the Runx2-DMR during the osteoblast differentiation (Fig. 4C). We found that upon osteoblast differentiation of MC3T3-E1 cells, mRNA level of DNA demethylation enzymes *Tet1* was significantly increased while that of *Tet3* was slightly decreased (Fig. S6). These changes of DNA demethylation enzyme expression could contribute to the DNA demethylation on the Runx2-DMR.

Next, we conducted a gene expression analysis of *Runx2* and its target genes, *Alpl* and *Osx*, in epigenome-edited cells. At Differentiation Day 0, no significant differences were observed in the mRNA levels of *Runx2* and its target genes between the "empty" and "pooled" samples (Fig. 4D). On the other hand, after 14 days of differentiation induction, we observed a significantly lower expression of *Runx2* in the "pooled" compared to the "empty", either in general *Runx2* mRNA or in the specific detection of *Runx2-I* (Fig. 4D). Nonetheless, no differences were observed in the expression of the *Alpl* and *Osx* between the "empty" and "pooled" (Fig. 4D). Finally, alizarin red S staining was performed after 14 days of differentiation induction and qualitative and quantitative analyses of the staining revealed no significant differences in the staining intensity between the "empty" and "pooled" samples (Fig. 4E and F). These results indicate that the induced epigenome editing of the Runx2-DMR successfully repressed the expression level of *Runx2*, despite the inhibitory effect being insufficient to suppress the downstream gene expression or the overall process of osteoblast differentiation.

4. Discussion

In this study, we demonstrated that the transient introduction of CRISPRoff and a pool of gRNAs could induce DNA hypermethylation to a T-DMR, consequently downregulating the gene expression of a nearby gene. Technically, the range and duration of DNA methylation achieved in our experiments were comparable to those reported in previous studies [16,18,27], but to our knowledge, this is one of the first reports of epigenome editing regulating DNA methylation of an endogenous T-DMR in association with its functional role [28,29].

Our results provide direct evidence that the epigenetic state of the Runx2-DMR has a causal relationship with *Runx2* expression, adding a novel layer to the regulation of the osteogenic master transcription factor. We observed a progressive DNA demethylation activity on the Runx2-DMR during osteoblast differentiation in MC3T3-E1 cells, expanding on previous knowledge from a study reporting a declining trend in DNA methylation levels of a specific CpG (CpG-2505) within this DMR during the osteoblast differentiation of mesenchymal stem cells (MSCs) [10]. The detailed mechanism of how DNA demethylation occurs in Runx2-DMR upon osteoblast differentiation remains elusive. Sepulveda et al. reported that during BMP2-triggered osteoblast differentiation of C3H10T1/2 mesenchymal cells, *Tet1/2* expression was increased and a Tet1-containing demethylation complex was recruited to the Sp7 promoter region, which resulted in DNA demethylation and increased *Sp7* expression [30]. As we also observed an increase in *Tet1* expression upon BMP2-triggered osteoblast differentiation (Fig. S6), a similar mechanism could take place in Runx2-DMR. Runx2-DMR, like other CpG island shores, is located at the boundary between the highly methylated intergenic region and the lowly methylated region, including a CpG island proximal to the TSS. CpG island shores have been reported to show differential DNA methylation levels in association with the transcriptional activity of the gene in the vicinity; thus, increased expression of a nearby gene may regulate the methylation level of the CpG island shore. It will be interesting to explore the possible positive-feedback relationship between Runx2 expression and Runx2-DMR DNA methylation in future studies. Altogether, the regulation of DNA methylation of the Runx2-DMR could be one of the endogenous regulatory mechanisms controlling *Runx2* expression during osteoblast differentiation. This aligns with the observations that the CpG island shores often exhibit tissue/cell-type-dependent DNA methylation regulation [13] as well as stochastic changes of DNA methylation levels [12], both of which result in transcriptional changes of the surrounding genes. Tissue/cell-type-dependent DNA methylation regulation is especially important for normal cellular differentiation and fetal development [31].

While we were able to modulate *Runx2* expression through epigenome editing, the expression of downstream RUNX2-target genes or osteogenic differentiation did not exhibit significant differences. This suggests that either the degree of epigenetic change was not sufficient, or the regulation exerted by DNA methylation at this T-DMR is fine-tuning in nature. *Runx2* has two TSS, and the proximity of this DMR to one of them (Runx2-I) may also influence the limitation. Nonetheless, epigenetic regulation through T-DMR may play a more substantial role under conditions where cells/organisms are sensitive to changes in Runx2 expression levels, such as in the regulation of the wild-type allele in haploinsufficient individuals. Of note, phenotypic differences in excessive teeth between identical twin CCD patients have been reported [32], suggesting that epigenetic mechanisms may play a role in the severity of CCD, probably through the quantitative regulation of Runx2. Experiments, such as conducting similar epigenome editing on the osteogenic differentiation of mesenchymal stem cells (MSCs) in *Runx2* heterozygous mice, could provide valuable insights in future studies.

CRediT authorship contribution statement

Yutaro Kawa: Writing – original draft, Data curation. **Miyuki Shindo:** Writing – review & editing, Data curation. **Jun Ohgane:** Writing – review & editing, Funding acquisition, Data curation, Conceptualization. **Masafumi Inui:** Writing – review & editing, Writing – original draft, Supervision, Data curation, Conceptualization.

Declaration of competing interest

The authors declare the following financial interests/personal relationships which may be considered as potential competing interests:

Masafumi Inui reports financial support was provided by Japan Society for the Promotion of Science. Jun Ohgane reports financial support was provided by Japan Society for the Promotion of Science. If there are other authors, they declare that they have no known competing financial interests or personal relationships that could have appeared to influence the work reported in this paper.

Data availability

Data will be made available on request.

Acknowledgements

This research was supported by the Ministry of Education, Culture, Sports, Science and Technology (MEXT) KAKENHI (21H04755 to J.O., 22H02636 and 21H04755 to M.I.)

Appendix A. Supplementary data

Supplementary data to this article can be found online at https://doi.org/10.1016/j.bbrep.2024.101733.

References

[1] T. Komori, Regulation of proliferation, differentiation and functions of osteoblasts by runx2, Int. J. Mol. Sci. 20 (2019) 1694.
[2] T. Komori, H. Yagi, S. Nomura, et al., Targeted disruption of Cbfa1 results in a complete lack of bone formation owing to maturational arrest of osteoblasts, Cell 89 (1997) 755–764.
[3] F. Otto, A.P. Thornell, T. Crompton, et al., Cbfa1, a candidate gene for cleidocranial dysplasia syndrome, is essential for osteoblast differentiation and bone development, Cell 89 (1997) 765–771.
[4] S. Mundlos, F. Otto, C. Mundlos, et al., Mutations involving the transcription factor CBFA1 cause cleidocranial dysplasia hereditary skeletal disorders comprise a large group, Cell 89 (1997) 773–779.
[5] W. Liu, S. Toyosawa, T. Furuichi, et al., Overexpression of Cbfa1 in osteoblasts inhibits osteoblast maturation and causes osteopenia with multiple fractures, J. Cell Biol. 155 (2001) 157–166.
[6] Y. Lou, A. Javed, S. Hussain, et al., A Runx2 threshold for the cleidocranial dysplasia phenotype, Hum. Mol. Genet. 18 (2009) 556–568.
[7] R. Mevel, J.E. Draper, M. Lie-A-Ling, et al., RUNX transcription factors: orchestrators of development, Development 146 (2019) dev148296.
[8] S.J. Rice, G. Aubourg, A.K. Sorial, et al., Identification of a novel, methylation-dependent, RUNX2 regulatory region associated with osteoarthritis risk, Hum. Mol. Genet. 27 (2018) 3464–3474.
[9] F. Wang, Y. Chen, J. Kong, et al., Differences of RUNX2 gene promoter methylation and transcription level in ankylosing spondylitis, Int. J. Rheum. Dis. 26 (2023) 2526–2533.
[10] S. Wakitani, D. Yokoi, Y. Hidaka, K. Nishino, The differentially DNA-methylated region responsible for expression of runt-related transcription factor 2, J. Vet. Med. Sci. 79 (2017) 230–237.
[11] R.A. Irizarry, C. Ladd-Acosta, B. Wen, et al., The human colon cancer methylome shows similar hypo- and hypermethylation at conserved tissue-specific CpG island shores, Nat. Genet. 41 (2009) 178–186.
[12] Y. Arai, K. Umeyama, N. Okazaki, et al., DNA methylation ambiguity in the Fibrillin-1 (FBN1) CpG island shore possibly involved in Marfan syndrome, Sci. Rep. 10 (2020) 5287.
[13] T. Imamura, J. Ohgane, S. Ito, et al., CpG island of rat sphingosine kinase-1 gene: tissue-dependent DNA methylation status and multiple alternative first exons, Genomics 76 (2001) 117–125.
[14] Y. Arai, K. Umeyama, K. Takeuchi, et al., Establishment of DNA methylation patterns of the Fibrillin1 (FBN1) gene in porcine embryos and tissues, J. Reprod. Dev. 63 (2017) 157–165.
[15] D. Bikard, W. Jiang, P. Samai, et al., Marraffini, Programmable repression and activation of bacterial gene expression using an engineered CRISPR-Cas system, Nucleic Acids Res. 41 (2013) 7429–7437.
[16] S. Morita, H. Noguchi, T. Horii, et al., Targeted DNA demethylation in vivo using dCas9-peptide repeat and scFv-TET1 catalytic domain fusions, Nat. Biotechnol. 34 (2016) 1060–1065.
[17] A. Amabile, A. Migliara, P. Capasso, et al., Inheritable silencing of endogenous genes by hit-and-run targeted epigenetic editing, Cell 167 (2016) 219–232.
[18] J.K. Nuñez, J. Chen, G.C. Pommier, et al., Genome-wide programmable transcriptional memory by CRISPR-based epigenome editing, Cell 184 (2021) 2503–2519.
[19] H. O'geen, M. Tomkova, J.A. Combs, et al., Determinants of heritable gene silencing for KRAB-dCas9 + DNMT3 and Ezh2-dCas9 + DNMT3 hit-and-run epigenome editing, Nucleic Acids Res. 50 (2022) 3239–3253.
[20] K. Fukunaga, M. Tanji, N. Hanzawa, et al., Protocadherin-1 is expressed in the notochord of mouse embryo but is dispensable for its formation, Biochem. Biophys. Rep. 27 (2021) 101047.
[21] L.-C. Li, R. Dahiya, MethPrimer: designing primers for methylation PCRs, Bioinformatics 18 (2002) 1427–1431.
[22] Y. Kumaki, M. Oda, M. Okano, QUMA: quantification tool for methylation analysis, Nucleic Acids Res. 36 (2008) W170–W175.
[23] M. Inui, M. Miyado, M. Igarashi, et al., Rapid generation of mouse models with defined point mutations by the CRISPR/Cas9 system, Sci. Rep. 4 (2014) 5396.
[24] P. Mali, L. Yang, K.M. Esvelt, et al., RNA-guided human Genome engineering via Cas9, Science 339 (2013) 819–823.
[25] Y. Naito, K. Hino, H. Bono, K. Ui-Tei, CRISPRdirect: software for designing CRISPR/Cas guide RNA with reduced off-target sites, Bioinformatics 31 (2015) 1120–1123.
[26] Y. Arai, H. Fukukawa, T. Atozi, et al., Ultra-deep bisulfite sequencing to detect specific DNA methylation patterns of minor cell types in heterogeneous cell populations: an example of the pituitary tissue, PLoS One 11 (2016) e0146498.
[27] A. Vojta, P. Dobrinić, V. Tadić, et al., Repurposing the CRISPR-Cas9 system for targeted DNA methylation, Nucleic Acids Res. 44 (2016) 5615–5628.
[28] T. Horii, S. Morita, S. Hino, et al., Successful generation of epigenetic disease model mice by targeted demethylation of the epigenome, Genome Biol. 21 (2020). Article number: 77.
[29] S. Kojima, N. Shiochi, K. Sato, et al., Epigenome editing reveals core DNA methylation for imprinting control in the Dlk1-Dio3 imprinted domain, Nucleic Acids Res. 50 (2022) 5080–5094.
[30] H. Sepulveda, A. Villagra, M. Montecino, Tet-mediated DNA demethylation is required for SWI/SNF-dependent chromatin remodeling and histone-modifying activities that trigger expression of the Sp7 osteoblast master gene during mesenchymal lineage commitment, Mol. Cell Biol. 37 (2017) e00177, 17.
[31] J. Ohgane, S. Yagi, K. Shiota, Epigenetics: the DNA methylation profile of tissue-dependent and differentially methylated regions in cells, Placenta 29 (2008) 29–35.
[32] N. Suda, M. Hattori, K. Kosaki, et al., Correlation between genotype and supernumerary tooth formation in cleidocranial dysplasia, Orthod. Craniofac. Res. 13 (2010) 197–202.